Photomagnetism in Cyano-Bridged Hexanuclear Clusters $[Mn^{II}(bpy)_2]_4[M^{IV}(CN)_8]_2 \cdot xH_2O$ (M = Mo, x = 14, and M = W, x = 9)

Corine Mathonière,*,† Robert Podgajny,‡ Philippe Guionneau,† Christine Labrugere,† and Barbara Sieklucka*,‡

ICMCB-CNRS, 87 avenue du Docteur Schweitzer, 33608 Pessac, France, and Faculty of Chemistry Jagiellonian University, Ingardena 3, 30-060 Krakow, Poland

Received July 26, 2004. Revised Manuscript Received November 9, 2004

The magnetic and photomagnetic properties of two cyano-bridged, $[Mn(bpy)_2]_4[Mo(CN)_8]_2 \cdot 14H_2O$ (**1**) and $[Mn(bpy)_2]_4[W(CN)_8]_2 \cdot 9H_2O$ (**2**) (bpy = 2,2′-bipyridyl), hexanuclear clusters (hereafter named $Mn^{II}_4M^{IV}_2$) have been investigated. Before irradiation both compounds behave as paramagnets in almost the whole temperature range due to the presence of magnetic Mn^{II} centers separated by the diamagnetic M^{IV} spacers in the molecules. After several hours of irradiation (337−356, 406−415, and 480 nm) in a superconducting quantum interference device at 10 K, the magnetic signal at 10 K has increased by a factor of almost 30% compared to that of the initial magnetic state. The magnetic characterization of the irradiated samples indicates the formation of a photoproduct exhibiting antiferromagnetic interactions. The X-ray photoelectron spectroscopy (XPS) data of the irradiated samples show the presence of Mn^{II}, Mn^{I}, M^{IV}, and M^{V} centers. The formation of Mn^{I} and M^{V} centers is interpreted in terms of the reductive quenching of the excited state through an intramolecular electron-transfer mechanism in the $Mn^{II}_4M^{IV}_2$ clusters. After irradiation at room temperature in the presence of air, both compounds behave as a paramagnet, but with a lower magnetic response than that of the initial state. The XPS data show the presence of M^{IV}, M^{VI}, and only Mn^{II} centers. The photochemical pathway in the presence of O_2 is discussed in relation to the *ligand-field* photochemistry of octacyanometalates(IV), leading ultimately to the formation of $[M^{VI}(CN)_4(O_2)]$ and low-spin $[Mn^{II}(bpy)_2(CN)_2]$ species in the solid state.

Introduction

The light-induced modification of the electronic properties is a challenging topic in material science in view of the possible application in optical and memory devices.[1] Supramolecular heterobimetallic coordination networks based on electronically active cationic 3d metal complexes and octacyanometalates of Mo and W building blocks are especially suitable for spin bistability function as the labile electronic configurations of metal centers may be changed reversibly involving magnetic, optical, and structural changes, stimulated by a variation of temperature and by light irradiation.

In 2000, one of us started systematic photomagnetic studies on octacyanometalate(IV)-based systems.[2] The light-induced modifications of magnetic properties were observed in Cu^{II}−NC−Mo^{IV} and Mn^{II}−NC−Mo^{IV} polymeric networks of various topologies.[2−6] The irradiation of 3-D $\{Cu^{II}_2[Mo^{IV}(CN)_8]\}$ with UV or visible light at low temperature induces the conversion to the metastable phase $\{Cu^{I}Cu^{II}[Mo^{V}(CN)_8]\}$, revealing ferromagnetic interaction between Cu^{II} and Mo^{V} centers.[3−6] A similar effect was recorded for 1-D $[Mn^{II}_2L_2(H_2O)_2][Mo^{IV}(CN)_8] \cdot 5H_2O$ (L = a macrocyclic ligand, 2,13-dimethyl-3,6,9,12,18-pentaazabicyclo[12.3.1]octadeca-1(18),2,12,14,16-pentaene).[2] Recently, the photomagnetic studies of 2-D $Cs^{I}\{[Co^{II}(3\text{-}CNpy)_2][W^{V}(CN)_8]\} \cdot H_2O$ have shown the *charge-transfer-induced spin transition* (CTIST) as well as *light-induced excited-spin-state trapping* (LIESST) between high-temperature (HT) $Co^{II}(S = 3/2)W^{V}(S = 1/2)$ (high-spin, HS) and low-temperature (LT) $Co^{III}(S = 0)W^{IV}(S = 0)$ (low-spin, LS) phases.[7]

However, the extended polymeric networks render difficult the quantitative interpretation of the photoinduced magnetic properties based on an analytical expression of the thermal dependence of $\chi_M T$, taking into account the exchange coupling in photoproducts, and also relaxation dynamics. The knowledge of these parameters is important in the design of new photomagnetic molecular materials with optimized properties. The discrete compounds offer the possibility to obtain simple coupling schemes, and therefore the determi-

* To whom correspondence should be addressed. E-mail: mathon@icmcb-bordeaux.cnrs.fr (C.M.); siekluck@chemia.uj.edu.pl (B.S.).
† ICMCB-CNRS.
‡ Faculty of Chemistry Jagiellonian University.

(1) Gutlich, P.; Garcia, Y.; Woike, T. *Coord. Chem. Rev.* **2001**, *219−221*, 839−879.
(2) Rombaut, G.; Golhen, S.; Ouahab, L.; Mathoniere, C.; Kahn O. *J. Chem. Soc., Dalton Trans.* **2000**, 3609.
(3) Ohkoshi, Sh.; Machida, N.; Zhong, Z. J.; Hashimoto, K. *Synth. Met.* **2001**, *122*, 523.
(4) Ohkoshi, Sh.; Machida, N.; Abe, Y.; Hashimoto, K. *Chem. Lett.* **2001**, 312.
(5) Rombaut, G.; Mathoniere, C.; Guionneau, P.; Gohlen, S.; Ouahab, L.; Verelst, M.; Lecante, P. *Inorg. Chim. Acta* **2001**, *326*, 27.
(6) Rombaut, G.; Verelst, M.; Golhen, S.; Ouahab, L.; Mathonière, C.; Kahn, O. *Inorg. Chem.* **2001**, *40*, 1151.
(7) Arimoto, Y.; Ohkoshi, Sh.; Zhong, Z. J.; Seino, H.; Mizobe, Y.; Hashimoto, K. *J. Am. Chem. Soc.* **2003**, *125*, 9240.

10.1021/cm048785l CCC: $30.25
Published on Web 12/30/2004

nation of the analytical parameters.

Only two examples of the photomagnetic studies of discrete bimetallic octacyanomolybdate(IV)-based molecules are known. The UV light irradiation of trinuclear $[Cu^{II}(bpy)_2]_2[Mo^{IV}(CN)_8]\cdot 5H_2O\cdot CH_3OH$ produces irreversibly $[Cu^{II}(bpy)_2]_2[Mo^{V}(CN)_8]\cdot 5H_2O\cdot CH_3OH$ characterized by antiferromagnetic coupling.[6] Very recently, we have investigated the photomagnetic properties of paramagnetic heptanuclear $[(tren)Cu^{II}]_6[Mo^{IV}(CN)_8](ClO_4)_8$ [tren = tris(2-aminoethyl)amine].[8] A blue visible light induces a *metal-to-metal charge-transfer* transition, leading to thermally reversible $Cu^{II}_6Mo^{IV} \leftrightarrow Cu^{II}_5Cu^{I}Mo^{V}$ photoredox conversion. The formation of the paramagnetic Mo^V with $S_{Mo} = 1/2$ induces Mo^V-Cu^{II} ferromagnetic interactions in $Cu^{II}_5Cu^{I}Mo^{V}$ at low temperatures, resulting in a final spin state $S = 3$. The photomagnetic effect is characterized by the amplitude measured as $\Delta\chi_M T = (\chi_M T)_{\text{after } h\nu} - (\chi_M T)_{\text{before } h\nu}$ equal to 2.5 $cm^3\ mol^{-1}$ K at 16 K. To increase the relative amplitude of the photomagnetic effect, we decided to investigate cyano-bridged bimetallic polynuclear molecules containing metal centers with spins higher than 1/2.

In this study we report the comparison of the structural features and photomagnetic properties of hexanuclear cyano-bridged $[Mn^{II}(bpy)_2]_4[M^{IV}(CN)_8]_2\cdot xH_2O$ [$Mn^{II}_4M^{IV}_2$; M = Mo, $x = 14$ (**1**); M = W, $x = 9$ (**2**)] clusters with four high-spin Mn^{II} centers of $S = 5/2$. The synthesis, spectroscopic characterizations, and single-crystal X-ray structure of $[Mn^{II}(bpy)_2]_4[Mo^{IV}(CN)_8]_2\cdot 14H_2O$ ($Mn^{II}_4Mo^{IV}_2$, **1**) have been reported by some of us.[9] The clusters are good candidates for exhibiting photoinduced magnetic properties, as they represent a variety of accessible oxidation states due to the photoredox character of the centers involved. To elucidate the mechanism responsible for the photoinduced magnetic effects, X-ray photoelectron spectroscopy (XPS) characterization of clusters and photoproducts has been performed. The results allow us to propose photochemical transformations leading to the observed photoinduced magnetic effects.

Experimental Section

Materials. The two title compounds were made according to a literature procedure.[9]

Physical Measurements. IR spectra were measured as KBr pellets on a Perkin-Elmer FT-IR Paragon 1000 spectrometer.

X-ray Studies. The room temperature powder X-ray diffraction pattern for **2** was recorded over the angular range $5° < 2\theta < 110°$ with a 0.02° step and a counting time of 10 s on a Philips PW 3040/00 X'PERT MPD device in Bragg−Brentano geometry using diffracted beam graphite monochromator Cu Kα radiation (λ = 1.5406 Å). Unit cell parameter values were derived from a peak indexation using DICVOL91.[10] The best solution to index all the observed Bragg reflections gives a satisfactory quality criterion: $M_{20} = 40$, $F_{20} = 127$ (0.0024, 66).

Magnetic and Photomagnetic Properties. The experiments were carried out with a Quantum Design MPMS-5S magnetometer working in the dc mode. The photomagnetic experiments were performed with a Kr^+ laser coupled through an optical fiber directed into the superconducting quantum interference device (SQUID) cavity. Powder samples were deposited onto a sample holder as thin layers (mass: 0.25 mg of **1** and 0.19 mg of **2**) to avoid surface effects during the irradiation. The diamagnetic contribution and the mass were estimated by comparing the magnetization **M** curves (vs magnetic field **H** and temperature *T*) before irradiation with the curves recorded in a routine magnetic experiment (4.6 mg of **1** and 20.1 mg of **2** of samples loaded into gel caps). The samples were irradiated continuously using three different multilines: 337−356, 406−415, and 480 nm under a magnetic field of 5 kOe at 10 K. The effective power of the laser beam employed was less than 10 mW/cm^2. Magnetic measurements were performed before and after irradiation, in each case the light being turned off to avoid thermal inhomogeneities. The dependence of magnetization on the temperature has been measured with the following steps: (i) determination of **M**(**H**) at 5 K followed by **M**(*T*) with a temperature increase of 5−300 K, (ii) cooling of the sample from 300 to 5 K (for 1.5 h) and determination of a new **M**(**H**) at 5 K followed by a new **M**(*T*) with a temperature increase of 5−300 K, and (iii) repetition of step ii.

Irradiations with the 337−356 nm laser line in ambient conditions (room temperature, presence of the air) have been performed for 15 h on a small weighted quantity of powder sample (0.8 mg) deposited on the bottom of a gel cap. Then the photoproducts have been magnetically characterized within a routine SQUID experiment.

XPS Experiments. XPS spectra were recorded with a 220i-XL ESCALAB from VG. Powder samples were pressed onto indium foils and put under UHV to reach the 10^{-8} Pa range. The nonmonochromatized Mg X-ray source was used at 200 W, as well as a flood gun to compensate for the nonconductive samples. The spectra were calibrated in relation to the C1s binding energy (284.6 eV), which was applied as an internal standard. Fitting of the high-resolution spectra was provided through the ECLIPSE program from VG.

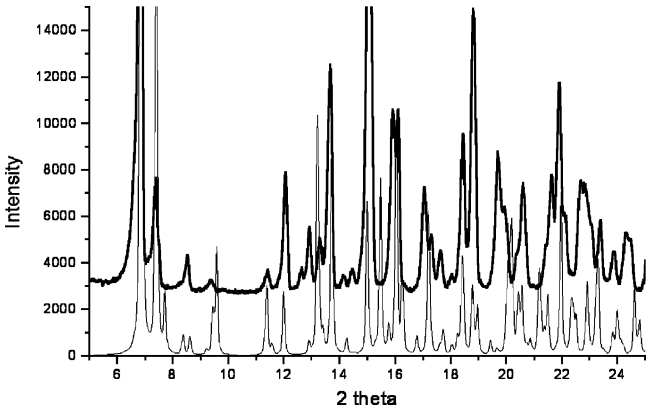

Figure 1. X-ray powder diffractogram for **2** (thick line) at 293 K and the simulated diffractogram for **1** from its single-crystal structure (thin line) determined at 180 K.

Results and Discussion

X-ray Powder Diffraction. The crystal structure of **1** is already known from single-crystal X-ray diffraction determination performed at 180 K.[9] The X-ray diffraction pattern of **1** has been simulated from the atomic positions and unit cell dimensions (a= 13.980(1) Å, b = 22.892(1) Å, c = 15.576(1) Å, β = 91.71(2)°, $P2_1/n$) contained in the Crystallography Information File (CIF, CSD code VEVVOH). Figure 1 compares the structural properties of **1** and

(8) Herrerra, J.-M.; Marvaud, V.; Verdaguer, M.; Marrot, J.; Kalisz. M.; Mathoniere, C. *Angew. Chem. Int. Ed. Engl.* **2004**, *43*, 5468.
(9) Sieklucka, B.; Szklarzewicz, J.; Kemp, T. J.; Errington, W. *Inorg. Chem.* **2000**, *39*, 5156.
(10) Boutlif, A.; Louer, D. *J. Appl. Crystallogr.* **1991**, *24*, 987.

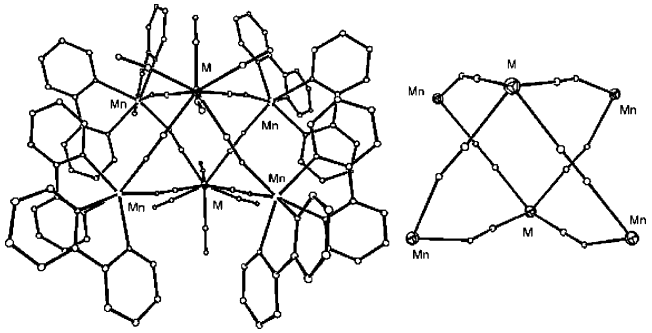

Figure 2. Molecular structure of the $[Mn^{II}(bpy)_2]_4[M^{IV}(CN)_8]_2$ cluster (left) and corresponding cyano-bridged $Mn^{II}_4M^{II}_2$ skeleton (right) in **1** and **2**.

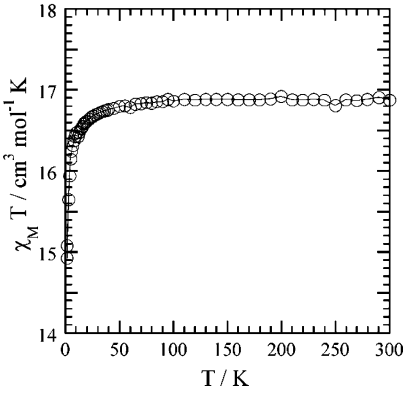

Figure 3. $\chi_M T$ vs T curve for **1**, $\mathbf{H} = 5$ kOe.

2. For **2**, the best solution to index all the observed Bragg reflections gives the monoclinic unit cell with $a = 13.863(2)$ Å, $b = 23.522(2)$ Å, $c = 15.409(3)$ Å, $\beta = 90.28(2)°$, and $V = 5024$ Å^3 with a satisfactory quality criterion: $M_{20} = 40$, $F_{20} = 127$ (0.0024, 66). Reflection conditions are consistent with the space group $P2_1/n$. Nevertheless, some differences either in relative intensity or in position are noted. These differences can be mainly attributed to thermal effects as the reported crystal structure has been determined at 180 K while the present powder pattern has been recorded at room temperature. Moreover, preferential orientation certainly affects the experimental pattern. Taking into account these features, we assume the similarity of the unit cells confirms that **1** and **2** are very close from a structural point of view. In conclusion, we can affirm that the molecular structure of **1** and **2** consists of a hexanuclear cluster with an octahedral geometry (Figure 2).[9] The Mo centers located at the almost orthogonal axis to the plane of the four Mn centers have four bridging and four terminal cyano ligands arranged in a square antiprism geometry. The molecule is realized by two, mutually perpendicular, $Mn^{II}_2M^{IV}_2$ squares, sharing the Mo for **1** (or W for **2**) corners. The Mn atoms are hexacoordinate, having a distorted octahedral geometry with two bpy ligands and two *cis* bent cyano bridges.

Magnetic Properties. The magnetic properties have been measured for both $Mn^{II}_4M^{IV}_2$ clusters. They are very similar, and we have chosen to present here the magnetic properties of **1**. Figure 3 shows the thermal dependence of the $\chi_M T$ product, where χ_M is the molar paramagnetic susceptibility and T is the temperature. In the high-temperature range (50−300 K), the $\chi_M T$ product is independent of the temperature and reaches a value of 16.90 cm^3 mol^{-1} K for **1** (17.6 cm^3 mol^{-1} K for **2**). These values are slightly different from the expected value of 17.5 cm^3 mol^{-1} K for four high-spin paramagnetic Mn^{II} centers, assuming $g = 2$. This can be explained by a g value different from 2 and the uncertainties of the water content (x) appearing during the purging before magnetic measurements. In the low-temperature range (5−50 K), the $\chi_M T$ product decreases with a decrease of temperature, reaching a value of 14.9 cm^3 mol^{-1} K at 5 K. Such behavior suggests weak antiferromagnetic interactions which may have two origins: probable intramolecular coupling between the Mn^{II} centers through bonds in the Mn^{II}−NC−M^{IV}−CN−Mn^{II} linkage (shortest Mn···Mn distance of 5.507 Å) or intermolecular interactions through space (shortest Mn−Mn distance of 7.56 Å). The **M**(**H**) curve measured at 1.84 K with magnetization at saturation, $\mathbf{M}_s$, equal to 20 Nβ shown in Figure 4 is close to the sum of four Brillouin functions with $S = 5/2$ with $g = 2$.

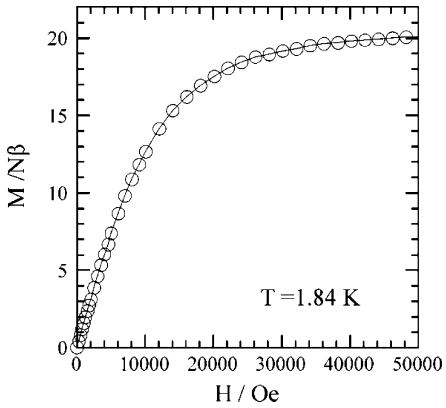

Figure 4. M vs **H** curve for **1**, $T = 1.84$ K.

Photomagnetic Properties of $Mn^{II}_4M^{IV}_2$ Clusters Irradiated in the SQUID at 10 K. The electronic solid-state reflectance spectra of **1** and **2** show the superposition of characteristic bands of the molecular precursors at 249, 300, and 410 (broad) and 540 (shoulder) nm for the Mo analogue and 249, 300, and 415 (broad) and 540 (shoulder) nm for the W analogue. The bands at 249 and 410 nm (or 415 nm) are assigned to the metal-to-ligand charge-transfer (MLCT) and d−d transitions in $[M(CN)_8]^{4-}$ units, respectively.[11] The band at 300 nm is assigned to intraligand (IL) $\pi-\pi^*$ transition of a coordinated bpy ligand in the $[Mn^{II}(bpy)_2(NC)_2]$ moiety. The shoulder near 540 nm is assignable to spin-forbidden d−d transition of the high-spin $[Mn^{II}(bpy)_2(NC)_2]$ chromophore.[12] Therefore, several wavelengths for irradiation of $Mn^{II}_4M^{IV}_2$ clusters in the SQUID cavity with a laser beam at 10 K have been tested (Table 1). The irradiation experiments at 337−356, 406−415, and 480 nm have revealed photomagnetic effects with a significant increase of the magnetic signal at 10 K. The irradiation at 647 nm showed no effect on the magnetic properties. This is consistent with the electronic spectra of the $Mn^{II}_4M^{IV}_2$ compounds.[9] To perform the detailed photomagnetic studies, we have chosen the 337−356 nm laser beam, in accord with the experiments leading to the photostationary state.

(11) Hendrickx, M. F. A.; Mironov, V. S.; Chirotu, L. F.; Ceuleumans, A. *Inorg. Chem.* **2004**, *43*, 3142.
(12) Lever, A. B. P. *Inorganic electronic spectroscopy*, 2nd ed.; Elsevier: New York, 1984; Chapter 6, pp 446−572.

Table 1. Photoexcitation Experiments Performed at 10 K in the SQUID (H = 5 kOe) for Clusters 1 and 2[a]

cluster	experiment no.	laser beam λ (nm)	photomagnetic effect: evolution of EMU	photomagnetic effect: photostationary state
1, $Mn^{II}_4Mo^{IV}_2$	1	406−415	increase	no
	2	336−357	increase	yes; $\Delta\chi_M T = 6$ cm^3 mol^{-1} K
	3	647	no effect	
2, $Mn^{II}_4W^{IV}_2$	1	336−357	increase	yes; $\Delta\chi_M T = 4$ cm^3 mol^{-1} K
	2	480	increase	no
	3	406−415	increase	no

[a] When a photostationary state is reached, the amplitude of the photomagnetic effect is given as $\Delta\chi_M T = (\chi_M T)_{\text{after } h\nu} - (\chi_M T)_{\text{before } h\nu}$; $(\chi_M T)_{\text{after hv}}$ is measured immediately after the laser beam is switched off.

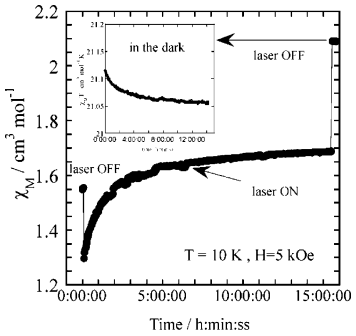

Figure 5. Time dependence of χ_M under 337−356 nm irradiation for **1**, $T = 10$ K, $\mathbf{H} = 5$ kOe. Inset: time dependence of $\chi_M T$ after the laser beam is switched off.

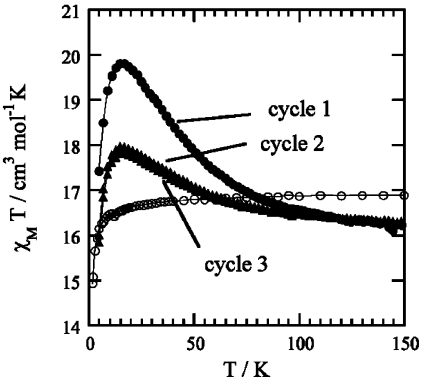

Figure 6. $\chi_M T$ vs T before irradiation (○) and after irradiation in cycles 1 (●) and 2 and 3 (▲) for **1**. For the description see the text.

The time dependence of the photomagnetic effect under irradiation with a 337−356 nm laser beam measured in the SQUID for **1** is shown in Figure 5. The value of χ_M (10 K, 5 kOe) increased from 1.55 cm^3 mol^{-1} before irradiation to 2.10 cm^3 mol^{-1} after irradiation, which corresponds to a net increase of 36%. Discontinuity at the starting and ending time points is due to the thermal heating caused by irradiation. The magnetic signal reaches a plateau after 16 h of irradiation. After the laser beam is switched off, the photoinduced signal remains almost unchanged, exhibiting 0.2% loss after 15 h at 10 K (Figure 5, inset). The thermal dependence of the photoinduced magnetic signal has been determined in three cycles as described in the Experimental Section (Figure 6). In the first cycle a change in character of the $\chi_M T$ vs T curve compared to that before irradiation has been observed: the $\chi_M T$ value increases from 17.4 cm^3 mol^{-1} K at 5 K, reaching a maximum of 19.85 cm^3 mol^{-1} K at 16 K, and then decreases to 16.5 cm^3 mol^{-1} K at 100 K. In the second cycle, the magnetic signal has the same character, but is significantly lower than the $\chi_M T$ vs T curve in the first cycle, with $\chi_M T$ values of 15.7, 17.97, and 16.22 cm^3 mol^{-1} K at 5, 16, and 150 K, respectively. In the third cycle the $\chi_M T$ vs T curve is almost superimposed on the previous one, with a $\chi_M T$ value of 16.11 cm^3 mol^{-1} K at 300 K. Finally, the three $\chi_M T$ curves are superimposed for $T > 110$ K. The incomplete relaxation during the first temperature increase indicates that the photoinduced modification of **1** is not reversible and leads to a new stable magnetic state of the cluster below 110 K (see below for further explanation). We have also noticed a change of color of the sample from pale yellow to dark brown after the irradiation.

To characterize the photoproduct, we have used XPS, which was a reliable tool for identification of oxidation states in compounds formed during the charge-transfer photochemistry of octacyanotungstate(V).[13] The XPS spectra of Mo3d binding energies of **1** before and after irradiation are shown in Figure 7. The XPS data concerning Mo3d binding energies of reference compounds $K_4[Mo^{IV}(CN)_8]$ and $Cs_3[Mo^{V}(CN)_8]$ and for **1** before and after irradiation are given in Table 2. The Mo3d spectrum of $K_4[Mo^{IV}(CN)_8]$ exhibits a doublet of binding energies 232.8 and 229.6 eV of $3d_{3/2}$ and $3d_{5/2}$ peaks with an intensity ratio of 0.64:1. The Mo3d spectrum of $Cs_3[Mo^{V}(CN)_8]$ exhibits two doublets, indicating the presence of nonequivalent Mo centers. The binding energies of the first doublet of 234.0 and 231.1 eV and the second one of 232.3 and 229.4 eV imply the presence of Mo^{V} and Mo^{IV} centers in the sample. The partial reduction of Mo^{V} to Mo^{IV} indicates that $Cs_3[Mo^{V}(CN)_8]$ is not stable under the X-ray beam with time. The Mo3d spectrum of **1** consists of one doublet of 232.8 and 229.6 eV with an intensity ratio of 0.64:1, consistent with the presence of Mo^{IV} centers. The Mo3d spectrum of **1** irradiated in the SQUID at 10 K consists of one doublet of 232.6 and 229.6 eV with an intensity ratio of 0.78:1. The substantial increase of the intensity of the Mo^{IV} $3d_{3/2}$ peak suggests the presence of a doublet assignable to the Mo^{V} center. We note also that the XPS spectrum evolves under the X-ray beam with time, which is consistent with the presence of unstable Mo^{V} centers. The XPS spectra of Mn2p binding energies of **1** before and after irradiation are shown in Figure 8. The Mn2p spectrum of **1** exhibits one doublet of 651.9 and 640.4 eV binding energies, characteristic of $Mn2p_{1/2}$ and $Mn2p_{3/2}$ peaks of Mn^{II}. The Mn2p spectrum of **1** irradiated in the SQUID at 10 K consists

(13) Sieklucka, B.; Dziembaj, R.; Witkowski, S. *Inorg. Chim. Acta* **1991**, *187*, 5.

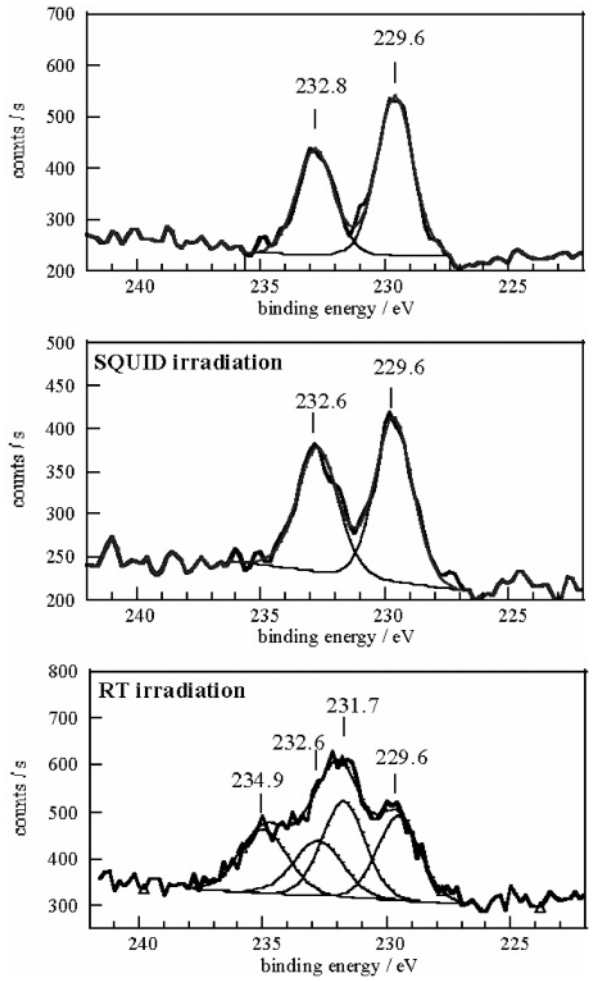

Figure 7. Mo3dXPS experimental and deconvoluted spectra for **1**: before irradiation (top), after irradiation in the SQUID (middle), and after irradiation in ambient conditions (bottom).

Table 2. XPS Spectral Parameters for Reference Compounds, Cluster 1, and Photoproducts of 1[a]

	Mo3d				
compound		BE (eV)	fwhm (eV)	ratio	assignment
$K_4[Mo(CN)_8]$	3/2	232.5	1.65	0.64	Mo^{IV}
	5/2	229.4	1.65	1	
$Cs_3[Mo(CN)_8]$	3/2	234.0	1.7	0.48	Mo^{V}
	5/2	231.1	1.6	0.76	Mo^{IV}
	3/2	232.3	1.7	0.64	
	5/2	229.4	1.7	1	
1	3/2	232.8	1.75	0.64	Mo^{IV}
	5/2	229.6	1.77	1	
1 irradiated in the SQUID	3/2	232.7	1.75	0.78	$Mo^{IV} + Mo^{V}$
	5/2	229.6	1.75	1	
1 irradiated in ambient conditions	3/2	234.9	2.35	0.73	$Mo^{VI} + Mo^{IV}$
	5/2	231.7	2.35	1.14	
	3/2	232.8	2	0.64	
	5/2	229.6	2	1	

[a] The doublet ratios have been calculated by comparison with the height of the $3d_{5/2}$ Mo^{IV} peak.

of a doublet of 650.9 and 639.4 eV binding energies. The shift of the Mn2p doublet by 1 eV to lower binding energies suggests the presence of Mn centers in two oxidation states which are ascribed to Mn^{II} and Mn^{I}. The XPS data of the $Mn^{II}_4Mo^{IV}_2$ cluster irradiated directly in the SQUID are

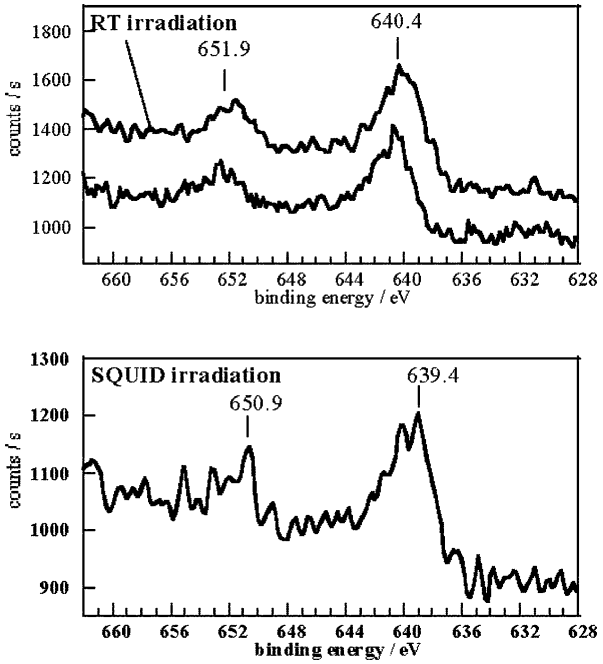

Figure 8. Mn2p XPS spectra for **1**: before and after irradiation in ambient conditions (top) and after irradiation in the SQUID (bottom).

consistent with the presence of Mo^{IV}, Mo^{V}, Mn^{II}, and Mn^{I} centers, indicating also the incomplete phototransformation of **1**.

The proposed mechanism of the photochemical reaction of the $Mn^{II}_4Mo^{IV}_2$ cluster at 10 K in the SQUID cavity involves a photoinduced electron transfer from Mo^{IV} to Mn^{II}, the $[Mn^{II}(bpy)_2]^{2+}$ serving as a light antenna. The excited $*[Mn^{II}(bpy)_2]^{2+}$ fragment is quenched via intramolecular reductive electron transfer by $[Mo(CN)_8]^{4-}$, resulting in formation of Mo^{V} and Mn^{I} centers. This interpretation is based on the assumption that the $*[Mn^{II}(bpy)_2]^{2+}$ site in $Mn^{II}_4Mo^{IV}_2$ is sufficiently long lived at 10 K and reductive quenching is thermodynamically favored. It is well-known that $[Mo(CN)_8]^{4-}$ serves as an effective quencher in reductive quenching of the excited state of, e.g., $[M(bpy)_3]^{n+}$ complexes of Cr^{III}, Ru^{II}, and Os^{III}, producing $[Mo(CN)_8]^{3-}$.[14,15]

The intramolecular reductive electron transfer in the excited $Mn^{II}_4Mo^{IV}_2$ cluster results in oxidation of the diamagnetic $Mo^{IV}(d^2, S = 0)$ center to the paramagnetic Mo^{V}-$(d^1, S = 1/2)$ center and the reduction of the paramagnetic $Mn^{II}(d,^5$ high spin, $S = 5/2)$ center to the paramagnetic Mn^{I}-$(d^6$, high spin, $S = 2)$ center. The photoproduct will have a $Mn^{II}_2Mn^{I}_2M^{V}_2$ metal center composition in the case of a 100% light conversion. Therefore, the magnetic interactions may appear in the $Mo^{V}-CN-Mn^{I}$ and $Mo^{V}-CN-Mn^{II}$ linkages. In the 1D $\{[Mn^{II}(bpy)(DMF)_2]_2[Mo^{V}(CN)_8]_2[Mn^{II}$-$(DMF)_4]\}$[16] and in the pentanuclear cluster $\{[Mn^{II}(bpy)_2]$-$[Mn^{II}(bpy)_2(H_2O)]_2[W^{V}(CN)_8]_2\}\cdot 7H_2O$[17] as well as in other

(14) Juris, A.; Gandolfi, M. T.; Manfrin, M. F.; Balzani, V. *J. Am. Chem. Soc.* **1976**, *98*, 1047.
(15) Juris, A.; Manfrin, M. F.; Maestri, M.; Serpone, N. *Inorg. Chem.* **1978**, *17*, 2258.
(16) Li, D.-F.; Gao, S.; Zheng, L.-M.; Tang, W. *J. Chem. Soc., Dalton Trans.* **2002**, 2805.
(17) Podgajny, R.; Desplanches, C.; Sieklucka, B.; Sessoli, R.; Villar, V.; Paulsen, C.; Wernsdorfer, W.; Dromzee, Y.; Verdaguer, M. *Inorg. Chem.* **2002**, *41*, 1323.

manganese(II) octacyanometalate(V)-based networks,[18] the $M^{V-}Mn^{II}$ interactions are antiferromagnetic. We assume therefore that the interactions in the $Mo^{V-}CN-Mn^{I}$ linkage in the photoproduct of **1** are also antiferromagnetic. If the photoconversion were complete, the spin ground state of the photoproduct molecule $Mn^{II}_2Mn^{I}_2Mo^{V}_2$ of $S = 8$ would give rise to a $\chi_M T$ value of 36 $cm^3\ mol^{-1}$ K at low temperature with $g = 2$. However, we can expect the quantum yield to be lower than unity by comparison with the efficiency of photoexcitation of mixed valence Prussian blue analogues during a SQUID experiment (less than 20% transformation of the powder sample).[19] Therefore, the magnetic properties of a solid sample of **1** after irradiation represent the sum of the magnetic contributions of the original cluster and photoproduct. Assuming that at 5 K only the spin ground state of the photoproduct is thermally populated, and neglecting intermolecular antiferromagnetic interactions between clusters, the low-temperature limit of $\chi_M T$ ($\chi_M T^{LT}$) at 5 K may be estimated with eq 1

$$(\chi_M T^{LT})_{calcd} = (1 - x)(\chi_M T^{LT})_{before} + x(\chi_M T^{LT})_{S=8} \quad (1)$$

where $(\chi_M T^{LT})_{before}$ is the $\chi_M T$ value of the original cluster before irradiation, $(\chi_M T^{LT})_{S=8}$ is the $\chi_M T$ value for the spin state $S = 8$ with $g = 2$, and x is the molar fraction of the photoproduct. The best estimation is obtained with $x = 0.12$ for the first cycle and $x = 0.05$ for the other two cycles (Figure 6). This means that the irradiated sample is composed of 12% $Mn^{II}_2Mn^{I}_2Mo^{V}_2$ and 88% $Mn^{II}_4Mo^{IV}_2$ during the first cycle and 5% $Mn^{II}_2Mn^{I}_2Mo^{V}_2$ and 95% $Mn^{II}_4Mo^{IV}_2$ during the other cycles. In general, the samples after irradiation are a mixture of the prevailing quantity of original $Mn^{II}_4M^{IV}_2$ and the small quantity of ferrimagnetic $Mn^{II}_2Mn^{I}_2M^{V}_2$ clusters. This is the main reason that the experimental $\chi_M T$ vs T curve does not exhibit the minimum of the $\chi_M T$ product characteristic for a ferrimagnetic system. In addition, the minimum is not well marked for systems containing high ($S = 5/2$) and low ($S = 1/2$) spins.[20] The previous description is valid if we consider that the system does not evolve with time. At 10 K, the relaxation is weak, with the loss of magnetic signal not exceeding 0.2% for 15 h. When the temperature is increased, the systems present magnetic properties depending on the thermal history. This suggests that the irradiation induces a two-step transformation. The first step involves the photoinduced formation of metastable state B from the initial state A (unirradiated $Mn^{II}_4M^{IV}_2$ cluster). In the second step the metastable state B undergoes

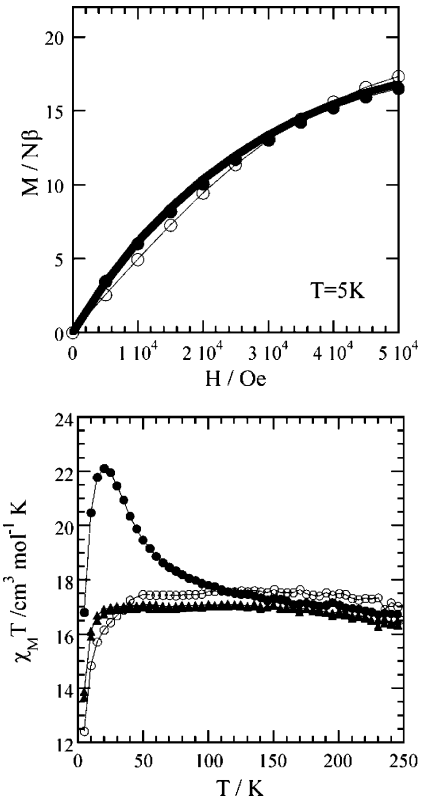

Figure 9. Top: **M** vs **H** curve before irradiation, $T = 5$ K (○), and after irradiation (●) and simulated **M** (thick line) with $x = 0.24$. Bottom: $\chi_M T$ vs T plots before irradiation (○) and after irradiation in cycles 1 (●) and 2 (▲) for **2**. For the description see the text.

a conversion to state C ($Mn^{II}_2Mn^{I}_2M^{V}_2$ photoproduct) with increased temperature:

$$A \xrightarrow[10\ K]{h\nu} B \xrightarrow{\Delta} C$$

The B and C states are not totally populated. The studied compounds are a mixture of A and B states at low temperature and a mixture of A and C states at temperatures above 110 K. Finally, the mixture of A and C states is stable with time. The magnetic signal of the C state is lower than that of the B state at low temperature. This can be explained in terms of a structural reorganization of metastable state B with increasing temperature, adjusting the bond lengths and angles of $[Mn(bpy)_2]$ fragments to the change of the oxidation state but not the magnetic composition of the photoproduct. The metric parameters of $[M(CN)_8]^{n-}$ ($n = 3, 4$) moieties in cyano-bridged networks are not diagnostic of the oxidation state of the M center.[21]

The $Mn^{II}_4W^{IV}_2$ cluster **2** exhibits a similar photomagnetic effect. Figure 9 (top) shows the effect of the irradiation as $\mathbf{M} = f(\mathbf{H})$ at 5 K. After irradiation, the magnetic signal has increased from the initial χ_M value of 1.56 $cm^3\ mol^{-1}$ to a χ_M value of 2.2 $cm^3\ mol^{-1}$. The new magnetization curve crosses the initial one at 3.25 T, showing higher values in the lower field region and lower values in the higher field region. The new saturation of 16.5 Nβ is lower than the 17.4 Nβ before irradiation. The shape of the magnetization curve

(18) See e.g.: (a) Zhong, Zh. J.; Seino, H.; Mizobe, Y.; Hidai, M.; Fujishima, A.; Ohkoshi, Sh., Hashimoto, K., *J. Am. Chem. Soc.* **2000**, *122*, 2952. (b) Zhong, Zh. J.; Seino, H.; Mizobe, Y.; Hidai, M.; Verdaguer, M.; Ohkoshi, Sh.; Hashimoto, K. *Inorg. Chem.* **2000**, *39*, 5095. (c) Song, Y.; Ohkoshi, Sh.; Arimoto, Y.; Seino, H.; Mizobe, Y.; Hashimoto, K. *Inorg. Chem.* **2003**, *42*, 1848. Li, D.; Zheng, L.; Zhang, Y.; Huang, J.; Gao, S.; Tang, W. *Inorg. Chem.* **2003**, *42*, 6123. (e) Pradhan, R.; Desplanches, C.; Guionneau, Ph.; Sutter, J.-P. *Inorg. Chem.* **2003**, *42*, 6607.

(19) Varret, F.; Nogues, M.; Goujon, A. In *Magnetism: molecules to materials*; Tome, I., Miller, J. S., Drillon, M., Eds.; VCH: New York, 2001; p 281.

(20) Pei, Y.; Journaux, Y.; Kahn, O.; Dei, A.; Gatteschi, D. *J. Chem. Soc., Chem. Commun.* **1986**, 1300.

(21) Podgajny, R.; Korzeniak, T.; Stadnicka, K.; Dromzee, Y.; Alcock, N. W.; Errington, W.; Kruczała, K.; Bałanda, M.; Kemp, T. J.; Verdaguer, M.; Sieklucka, B. *Dalton Trans.* **2003**, 3458 and references therein.

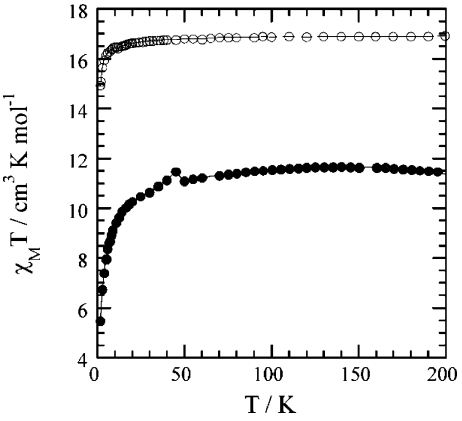

Figure 10. $\chi_M T$ vs T plot before (○) and after (●) irradiation in ambient conditions for **1**.

after irradiation indicates the formation of the photoproduct with ferrimagnetic interactions. As in the previous case the magnetization can be simulated using eq 2

$$\mathbf{M}_{\text{calcd}} = (1 - x)\mathbf{M}_{\text{before}} + x\mathbf{M}_{S=8} \qquad (2)$$

where $\mathbf{M}_{\text{before}}$ is the magnetization of the original cluster before irradiation, $\mathbf{M}_{S=8}$ is the Brillouin function with spin state $S = 8$ with $g = 2$, and x is the molar fraction of the photoproduct. The best simulation is obtained with $x = 0.24$. Therefore, the irradiated sample is composed of 24% $Mn^{II}{}_2Mn^{I}{}_2W^{V}{}_2$ and 76% $Mn^{II}{}_4W^{IV}{}_2$ at low temperature. The thermal dependence of the photoinduced magnetic signal has been determined in three cycles as described in the Experimental Section (Figure 9, bottom). The character of the $\chi_M T$ versus T curve obtained in the first cycle resembles the character of the appropriate curve for **1** (see Figure 6, cycle 1). The maximum of the $\chi_M T$ product of 22.25 cm^3 mol^{-1} K is observed at 20 K. Generally, after irradiation the sample has a higher magnetic response in the low-temperature range ($T < 100$ K) and a lower magnetic response at higher temperature ($T > 120$ K). Such a profile of the $\chi_M T$ vs T curve confirms the formation of an exchange-coupled system. The $\chi_M T$ vs T curve recorded in the second cycle is close to the original one, indicating the loss of magnetic interactions between Mn and W centers and reversibility of the overall photochemical process.

Photomagnetic Properties of the $Mn^{II}{}_4Mo^{IV}{}_2$ Cluster Irradiated in Ambient Conditions. The irreversibility of the photomagnetic properties of **1** above 100 K has prompted us to investigate its photoreactivity in ambient conditions with a 337−356 nm laser beam. Figure 10 shows the $\chi_M T$ versus T curves before and after irradiation of **1**. After irradiation, the compound behaves as a paramagnet in the 50−300K range, but with a lower Curie plateau at 11.5 cm^3 mol^{-1} K compared to 16.9 cm^3 mol^{-1} K, indicating spin and/or structural changes.

The XPS data of Mo3d binding energies of **1** after irradiation in ambient conditions are shown in Table 2 and Figure 7 (bottom). The Mo3d spectrum is deconvoluted as an overlap of two doublets, indicating the presence of two oxidation state Mo centers. The binding energies of the first doublet of 232.6 and 229.6 eV are characteristic of Mo^{IV}. The binding energies of the second doublet of 234.9 and 231.7 eV can be assigned to Mo^{VI}.[22] The XPS spectrum of the Mn2p binding energies of **1** after irradiation is shown in Figure 8 (top). The Mn2p spectrum exhibits one doublet of 651.9 and 640.4 eV binding energies, characteristic of $Mn2p_{1/2}$ and $Mn2p_{3/2}$ peaks of Mn^{II}. The XPS data for **1** after irradiation in aerobic conditions at room temperature show clearly the presence of Mn^{II} and Mo^{IV} and the formation of Mo^{VI} centers.

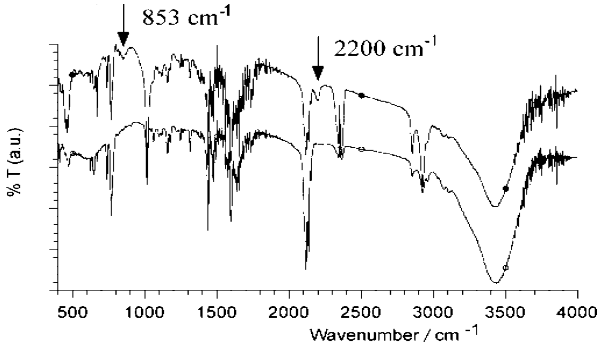

Figure 11. IR spectra of **1** unirradiated (○, bottom) and irradiated in ambient conditions (●, top). The arrows show the presence of new bands in **1** after irradiation.

To complete the characterization of **1** irradiated under ambient conditions, the IR spectra have been recorded (Figure 11). The two new bands at 853 and 2200 cm^{-1} appear after the irradiation. The frequency of 853 cm^{-1} is characteristic of a stretching vibration of a peroxo group with a side-on coordination to cyanomolybdenum(VI) compounds.[23,24] The 2200 cm^{-1} band can be assigned to the cyano stretching vibrations of terminal cyano ligands at M^{VI} centers.[23−26] It appears at higher energy compared to the terminal ν(CN) bands at M^{IV} and M^{V} centers. This is consistent with an increase of the oxidation state of the Mo, resulting in a decrease of π-back-donation, which shifts the CN stretching band toward higher energy.

The interpretation of the XPS and IR data for the aerobic irradiation of the $Mn^{II}{}_4Mo^{IV}{}_2$ cluster can be associated with the photodissociation of Mo−CN bonds in Mo−CN−Mn linkages, leading to the formation of $\{Mo^{IV}(CN)_4\}$ and $[Mn^{II}(bipy)_2(NC)_2]$ fragments in the primary photochemical step. The attack of dioxygen (O_2) on coordinatively unsaturated $\{Mo^{IV}(CN)_4\}$ species results in the formation of $[Mo^{VI}(CN)_4(O_2)]$ units.[23,24] The oxidation of the diamagnetic $Mo^{IV}(d^2, S = 0)$ to $Mo^{VI}(d^0, S = 0)$ does not modify the magnetic properties. The decrease of the magnetic signal after irradiation may have two origins: a spin change of the Mn^{II} centers and/or a structural change of the $[Mn^{II}(bipy)_2(NC)_2]$ fragments. The magnetic properties may be interpreted assuming the presence of the fraction of Mn^{II} centers in a low-spin configuration ($d,^5$ $S = 1/2$). The low-spin configuration may be attributed to the $[Mn^{II}(bipy)_2(CN)_2]$ unit, achieved by the

(22) Briggs, D.; Seah, M. P. *Practical surface analysis, Vol. 1: Auger and X-ray photoelectron spectroscopy*, 2nd ed.; VCH: New York, 1995.
(23) Matoga, D.; Szklarzewicz, J.; Samotus, A.; Burgess, J.; Fawcett, J.; Russel, D. R. *Polyhedron* **2000**, *19*, 1503.
(24) Matoga, D.; Szklarzewicz, J.; Samotus, A.; Lewiński, K. *J. Chem. Soc., Dalton Trans.* **2002**, 3587.
(25) Sieklucka, B.; Alcock, N. W.; Kemp, T. J.; Vincze, L.; Stufkens, D. J. *Inorg. Chim. Acta* **1989**, *163*, 127.
(26) Sieklucka, B.; Alcock, N. W.; Kemp, T. J.; Stufkens, D. J. *J. Chem. Soc., Dalton Trans.* **1990**, 2331.

Scheme 1. Energy Diagram Showing the Pathways of the Photoproduct Formation

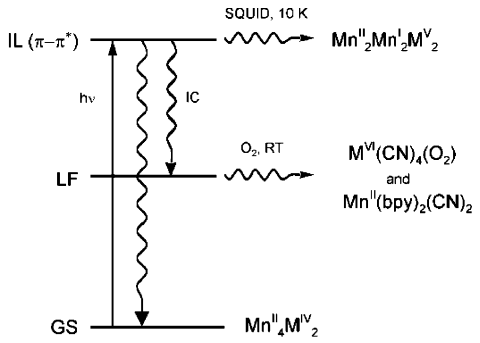

linkage isomerization of two cyano groups in the primary $[Mn^{II}(bipy)_2(NC)_2]$ fragment,[27,28] inducing the change of spin due to a stronger ligand field.

Conclusions

The two cyano-bridged $[Mn(bpy)_2]_4[Mo(CN)_8]_2 \cdot 14H_2O$ (**1**) and $[Mn(bpy)_2]_4[W(CN)_8]_2 \cdot 9H_2O$ (**2**) hexanuclear clusters exhibit photomagnetic properties strongly dependent on the experimental conditions employed. The irradiation within the $\pi-\pi^*$ IL of the bpy band at 10 K in the SQUID cavity and in ambient conditions leads to the different photochemical pathways and various photoproducts. The photoreactivity of $Mn^{II}_4M^{IV}_2$ clusters can be rationalized in terms of the mechanism given in Scheme 1. Irradiation of the $Mn^{II}_4M^{IV}_2$ cluster at 10 K in the SQUID cavity involves a long-lived $\pi-\pi^*$ IL state as the reactive lowest electronic excited state (LEES). The excited $*[Mn^{II}(bpy)_2]^{2+}$ fragment is quenched via intramolecular reductive electron transfer by $[Mo(CN)_8]^{4-}$, resulting in formation of Mo^V and Mn^I centers. The ambient conditions significantly shorten the lifetime of the excited CT state of the $[Mn(bpy)_2]^{2+}$ moiety, which by internal conversion (IC) undergoes decay to the photodissociative ligand-field (LF) state of the $[M(CN)_8]^{4-}$ fragment as the LEES. The photochemical process can be associated with the photodissociation of Mo−CN bonds in Mo−CN−Mn linkages, leading to the formation of $\{M^{IV}(CN)_4\}$ and $[Mn^{II}(bipy)_2(NC)_2]$ fragments in the primary photochemical step. The attack of O_2 on coordinatively unsaturated $\{M^{IV}(CN)_4\}$ species results in the formation of $[M^{VI}(CN)_4(O_2)]$ units. The unstable $[Mn^{II}(bipy)_2(NC)_2]$ fragment undergoes linkage isomerization of N-coordinated cyano ligands to $[Mn^{II}(bipy)_2(CN)_2]$ of low-spin configuration. This study demonstrates that the photomagnetic properties of $Mn^{II}_4Mo^{IV}_2$ and $Mn^{II}_4W^{IV}_2$ clusters are comparable. The main difference lies in the pronounced reversibility of the $Mn^{II}_2Mn^{I}_2W^{V}_2$ system due to the lower redox potential of the $[W(CN)_8]^{3-/4-}$ couple compared to the $[Mo(CN)_8]^{3-/4-}$ couple.[29] This work shows that the amplitude of the photomagnetic effect of 3.25 $cm^3\ mol^{-1}$ K for **1** at 16 K and 6.00 $cm^3\ mol^{-1}$ K for **2** at 20 K has been improved compared to 2.5 $cm^3\ mol^{-1}$ K obtained for heptanuclear $[(tren)Cu^{II}]_6[Mo^{IV}(CN)_8](ClO_4)_8$.[8] The photomagnetic studies of polynuclear clusters containing more metallic centers to increase significantly the photomagnetic effect are in progress.

Acknowledgment. The present research is supported in part by "Polonium" Polish-French Programme No. 05730UK and the State Committee for Scientific Research in Poland (KBN) (Grant No. 3T09A 15126).

CM048785L

(27) Bignozzi, C. A.; Chiorboli, C.; Indelli, M. T.; Scandola, F.; Bertolasi, V.; Gilli, G. *J. Chem. Soc., Dalton Trans.* **1994**, 2391.
(28) Anderson, K. M.; Connelly, N. G.; Llamas-Rey, E.; Orpen, G.; Paul, R. L. *J. Chem. Soc., Chem. Commun.* **2001**, 1734.
(29) Samotus, A.; Szklarzewicz, J. *Coord. Chem. Rev.* **1993**, *125*, 63.